Monthly Notices
of the
ROYAL ASTRONOMICAL SOCIETY

MNRASL **438,** L101–L105 (2014)
Advance Access publication 2013 December 20

doi:10.1093/mnrasl/slt171

The first month of evolution of the slow-rising Type IIP SN 2013ej in M74*

S. Valenti,[1,2]† D. Sand,[3] A. Pastorello,[4] M. L. Graham,[1,2] D. A. Howell,[1,2] J. T. Parrent,[1,5] L. Tomasella,[4] P. Ochner,[4] M. Fraser,[6] S. Benetti,[4] F. Yuan,[7] S. J. Smartt,[6] J. R. Maund,[6] I. Arcavi,[8] A. Gal-Yam,[8] C. Inserra[6] and D. Young[6]

[1]*Las Cumbres Observatory Global Telescope Network, 6740 Cortona Dr., Suite 102, Goleta, CA 93117, USA*
[2]*Department of Physics, University of California, Santa Barbara, Broida Hall, Mail Code 9530, Santa Barbara, CA 93106-9530, USA*
[3]*Physics Department, Texas Tech University, Lubbock, TX 79409, USA*
[4]*INAF – Osservatorio Astronomico di Padova, Vicolo dell'Osservatorio 5, I-35122 Padova, Italy*
[5]*Department of Physics and Astronomy, Dartmouth College, 6127 Wilder Laboratory, Hanover, NH 03755, USA*
[6]*Astrophysics Research Centre, School of Mathematics and Physics, Queens University Belfast, Belfast BT7 1NN, UK*
[7]*Research School of Astronomy and Astrophysics, The Australian National University, Weston Creek, ACT 2611, Australia*
[8]*Department of Particle Physics and Astrophysics, The Weizmann Institute of Science, Rehovot 76100, Israel*

Accepted 2013 November 25. Received 2013 November 25; in original form 2013 September 16

ABSTRACT

We present early photometric and spectroscopic observations of SN 2013ej, a bright Type IIP supernova (SN) in M74. SN 2013ej is one of the closest SNe ever discovered. The available archive images and the early discovery help to constrain the nature of its progenitor. The earliest detection of this explosion was on 2013 July 24.125 UT and our spectroscopic monitoring with the FLOYDS spectrographs began on July 27.7 UT, continuing almost daily for two weeks. Daily optical photometric monitoring was achieved with the 1 m telescopes of the Las Cumbres Observatory Global Telescope (LCOGT) network, and was complemented by UV data from *Swift* and near-infrared spectra from Public ESO Spectroscopic Survey of Transient Objects and Infrared Telescope Facility. The data from our monitoring campaign show that SN 2013ej experienced a 10 d rise before entering into a well-defined plateau phase. This unusually long rise time for a Type IIP has been seen previously in SN 2006bp and SN 2009bw. A relatively rare strong absorption blueward of Hα is present since our earliest spectrum. We identify this feature as Si II, rather than high-velocity Hα as sometimes reported in the literature.

Key words: supernovae: general – supernovae individual: SN 2013ej.

1 INTRODUCTION

Type IIP supernovae (SNe IIP) have been widely studied in the past. They arise from progenitors that have retained their hydrogen and helium layers before exploding as core-collapse (CC) SNe. Several progenitors of SNe IIP have been detected in archive images (see Smartt 2009 for a review). These SNe are also used as standard candles for cosmological studies (Hamuy 2001). For this reason it is important to investigate their diversity when new close-by SNe II are discovered. We have this opportunity with SN 2013ej, a young SN recently discovered in M74 (NGC 628).

SN 2013ej was discovered by the Lick Observatory Supernova Search on 2013 July 25.45 UT, with the 0.76 m Katzman Automatic Imaging Telescope. The coordinates of the SN are $\alpha = 01^{\rm h}36^{\rm m}48\overset{\rm s}{.}16$, $\delta = +15^\circ45'31\overset{''}{.}0$ (Kim et al. 2013). Pre-discovery detections on July 25.38 and on July 24.125 were also reported by Dhungana et al. (2013) with the 0.45 m ROTSE-IIIb telescope at McDonald Observatory and by C. Feliciano on the *Bright Supernovae*[1] website. The SN was caught extremely young, as a non-detection was reported by the All Sky Automated Survey for Supernovae (Shappee et al. 2013) on July 23.54 UT,[2] less than 1 d prior to the first detection, with a limit of $V > 16.7$ mag. We immediately triggered the robotic FLOYDS spectrograph mounted on the Faulkes Telescope South (FTS) at Siding Spring Observatory and were able to classify the transient on Jul. 27.7 UT as a young SN II (Valenti et al. 2013). Located $92\overset{''}{.}5$E, $135''$S from the core of

*This Letter is based on observations obtained with the following telescopes: LCOGT network of 1 and 2 m telescopes, NTT (184.D-1140,188.D-3003) and IRTF.

† E-mail: svalenti@lcogt.net

[1] http://www.rochesterastronomy.org/snimages/

[2] We will use JD = 245 6497.45$^{+4\,\rm h}_{-12\,\rm h}$ as the reference date for the shock breakout (see Section 3.2).

M74,[3] SN 2013ej is a very nearby SN. We note that M74 hosted two other CC SNe, namely SN 2002ap (SN Ic) and SN 2003gd (SN IIP).

Deep, high-esolution images of the host galaxy have been taken prior to the explosion of SN 2013ej using the *Hubble Space Telescope* (*HST*) and Gemini telescope. An analysis of these together with the identification and characterization of a progenitor star is presented in a companion paper (Fraser et al. 2013). A bright source in both the *HST* and Gemini images is identified by Fraser et al. (2013) as coincident with the position of SN 2013ej. The object is detected from the *U* to the *i* bands and does not have the colours of a single stellar source. Fraser et al. (2013) show that it is likely a blend of two, physically unrelated, stars. Assuming that the progenitor was a red supergiant (RSG), as found for other SNe IIP, then the progenitor zero-age main sequence mass would lie in the range 8–16 $M_{\odot}$. For the reasons mentioned above, SN 2013ej was promoted as a high-priority target for Las Cumbres Observatory Global Telescope (LCOGT)'s ongoing, intensive effort to obtain high-cadence optical photometry and spectroscopy of transient objects. A detailed overview of the LCOGT facilities can be found in Brown et al. (2013). Along similar lines, SN 2013ej was also monitored by the PESSTO[4] collaboration.

2 OBSERVATIONS

Spectroscopic follow-up of SN 2013ej was primarily obtained using the twin FLOYDS spectrographs on FTS and the Faulkes Telescope North, at Haleakala, with an ∼1 d cadence. FLOYDS has a prism cross-disperser which images first and second orders on to the chip, resulting in a very broad wavelength coverage of ∼3200–10 000 Å. Optical spectra were also obtained at the Asiago 1.22 m telescope with the B&C spectrograph. All optical spectra were reduced using standard IRAF routines. A higher resolution spectrum was obtained on August 23 with the 1.82 m Copernico telescope (Mt. Ekar, Asiago) equipped with an echelle spectrograph. Two near-infrared (NIR) spectra were also collected. A very early NIR spectrum (taken earlier than our first optical spectrum) was obtained with SpeX (Rayner et al. 2003) on the NASA Infrared Telescope Facility (IRTF). The SpeX data were reduced with the custom SPEXTOOL package (Cushing, Vacca & Rayner 2004), and were corrected for telluric absorption with the software and prescription of Vacca, Cushing & Rayner (2003). SOFI data were obtained during a PESSTO night and reduced with the PESSTO pipeline (Smartt et al., in preparation) (data available on WISeREP, see Table 1 in the supplementary material).

Optical (*UBVRIgriz*) photometric follow-up of SN 2013ej was obtained with the nine 1 m telescopes of the LCOGT network, and in this Letter we present data obtained up to one month after the SN discovery (data in Table 2 of the supplementary material). The data were reduced using a custom pipeline[5] developed by the LCOGT SN team. Additionally, *Swift* data of SN 2013ej with the Ultraviolet/Optical Telescope (Roming et al. 2005) were taken starting on 2013 July 30.87 UT. *Swift* photometry, going from the *uw2* filter through the *V* filter, has been measured using an aperture of 3 arcsec, and following the approach of Brown et al. (2009).

3 ANALYSIS AND RESULTS

3.1 Spectroscopy

The sequence of spectra collected for SN 2013ej is shown in Fig. 1(a). In analogy with canonical SNe II, at very early phases the spectra of SN 2013ej show a blue, almost featureless continuum. As the ejecta expand, the photospheric temperature declines, and a number of spectral lines appear, showing P-Cygni profiles that become more prominent with time. The earliest spectrum shows a blue continuum, with a blackbody temperature of 15 000 K. Together with weak and shallow Balmer-series lines, N II and He I likely contribute to the absorption features at 5550 and 5700 Å. From very early phases, an absorption feature on the blue side of Hα is detected (see Fig. 1c). This feature, observed in several young SNe II, has been widely discussed in the past, particularly for the classic Type IIP SN 1999em. The two identifications proposed to explain the dip are a high-velocity (HV) component of Hα (at ∼16 000 km s^{-1}) and Si II 6355 Å. The evolution of this feature has been observed in several IIP SNe (SN 2005cs, Pastorello et al. 2006; SN 2006bp, Quimby et al. 2007; SN 2009bw, Inserra et al. 2012; SN 2012A, Tomasella et al. 2013). It appears a few days after the shock breakout; it reaches a maximum intensity at around three weeks after maximum light before eventually fading. In Fig. 1(d) spectra at these three different epochs of SN 2013ej are compared with those of other SNe IIP (a few days, two weeks and three to four weeks after the explosion, respectively). In SN 1999em this absorption was visible since about one week post-explosion, and remained detectable for one additional week. Leonard et al. (2002) identified this absorption at early phases as Si II, while Baron et al. (2000) favoured an HV hydrogen interpretation. Inserra et al. (2012) also interpreted this feature as an HV hydrogen line in the Type II SN 2009bw.

Chugai, Chevalier & Utrobin (2007), on the other hand, proposed a time-dependent, dual interpretation. These authors attributed the shallow absorption in the Hα blue wing visible at early phases in SNe IIP to Si II, but a similar blueshifted notch seen at late times to HV hydrogen. Indeed, the interaction with a typical RSG wind should result in the enhanced excitation of the outer layers of unshocked ejecta and the emergence of corresponding HV absorption (see also Leonard et al. 2002 for a similar conclusion). In the case of SN 2013ej, we note a similar evolution of this absorption feature to previous works, although a notch is visible in our first spectrum and becomes stronger with time. At day +17 the blueshifted absorption is deeper than the regular Hα absorption. We also note that a similar feature is not visible in the blue wing of Hβ (see Fig. 1b), as one would expect if it were due to HV hydrogen.

In order to confidently exclude the HV H interpretation for the 6100 Å feature, we also present in Fig. 1(f) two NIR spectra obtained on July 27 and August 17. The first SpeX spectrum (+3.6^{d}) is one of the earliest NIR spectra ever published for an SN IIP. This shows a blue continuum, in addition in which only very shallow Paschen lines are detected. These become more prominent in the second spectrum, and show a broad absorption in Pa-γ (see the inset of Fig. 1f). While the red wing of the absorption is consistent with Pa-γ at ∼8000 km s^{-1} consistent with other hydrogen lines, the origin of the blue wing of this feature must wait for future work with time-series NIR spectroscopy. HV Pa-γ at ∼15 000 km s^{-1}

[3] A distance modulus of 29.79 mag (Fraser et al. 2013), or 9.1 Mpc, is used in this Letter.
[4] Public ESO Spectroscopic Survey of Transient Objects, www.pessto.org/
[5] The pipeline employs standard procedures (PYRAF, DAOPHOT, SWARP) in a PYTHON framework. Point spread function magnitudes were transformed to the standard Sloan Digital Sky Survey filter system (for *griz*) or Landolt (1992) system (for *UBVRI*) via standard star observations taken during clear nights.

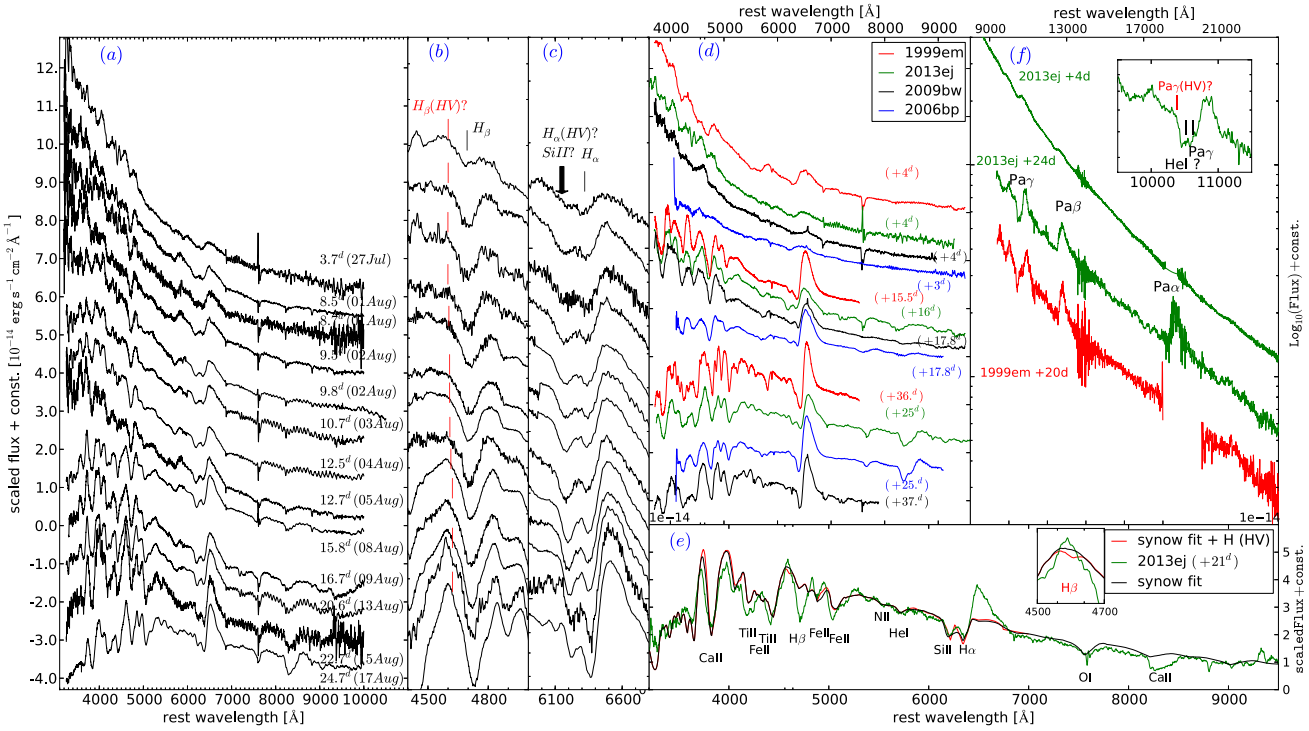

Figure 1. (a) Spectra series of SN 2013ej. (b) Hβ evolution. (c) Hα evolution. (d) Comparison of spectra of SN 2013ej with those of other SNe II at three different epochs. (e) Line identification: comparison between an observed spectrum of SN 2013ej (phase $+20^{\rm d}$) and a spectral model obtained using *synow* (see the text). (f) Infrared spectra of SN 2013ej and comparison with an early-phase spectrum of SN 1999em. The insert shows a detail of Pa-γ.

(as suggested by the HV hydrogen identification in the optical) can be excluded.

A *synow* (Fisher 2000) fit of the spectrum at 21 d is shown in Fig. 1(e), and the comparison model was obtained with the following contributing ions: Fe II, Ti II, He I, H I, O I, Si II, Ca II and N II. The Hβ mismatch is due to *synow*'s local thermodynamic equilibrium assumptions (see Dessart & Hillier 2010). Adding Si II nicely reproduces the feature on the blue side of Hα with no significant change in the *synow* spectrum due to other Si II lines. A *synow* fit using HV hydrogen is also shown with HV Hβ highlighted in the inset panel. Also remarkable are the Fe II lines, first detected when the temperature goes below 9000 K (as suggested by Dessart & Hillier 2006). In particular, the Fe II line at λ5166 appears two weeks after the shock breakout and is clearly detected one week later. In Fig. 2(a), we show the photospheric velocity where lines of different ions are forming. The velocity obtained for the Si II identification is also consistent with those of other elements.

3.2 Light curve

The light curve of SN 2013ej in the *uw*2, *um*2, *uw*1 and *UBVRIgriz* filters is shown in Fig. 2(b). SN 2013ej shows in all bands a relatively slow luminosity rise to the plateau. SNe II usually have a very fast rising lasting very few days. Through the comparison of the early light curve of SN 2010id with that of SN 2006bp (Quimby et al. 2007), Gal-Yam et al. (2011) suggested a variety in the rising time of SNe II, with some objects showing a slow rise. Another SN II with a slow rise to peak is SN 2009bw (Inserra et al. 2012). These three SNe are all quite bright (M_R between -17 and -18 at peak; see Fig. 2c). In particular, SN 2009bw is almost identical to SN 2013ej in the light-curve shape and the absolute magnitude (see Fig. 2b). The slow rising of these SNe lasting several days may be either related to the density structure of the outermost layers of the progenitor or to a significant contribution from the radioactive heating (instead of recombination heating) as usually seen in SNe IIb.

3.3 Progenitor radius

In CC SNe, soon after the shock breakout, the shock-heated envelope expands and cools down with different time-scales depending on the initial progenitor radius, opacity and gas composition. Simple analytic functions have been developed (Waxman, Meszaros & Campana 2007; Chevalier & Irwin 2011; Rabinak & Waxman 2011) to give a rough estimate of the radius of the progenitor of CC SNe using the temperature evolution at early phases. For instance, the SN photosphere after the explosion of an RSG remains at a higher temperature for a longer time than what occurs in a more compact blue supergiant (BSG). Making use of our spectrophotometric data within one week from the shock breakout and equation 13 of Rabinak & Waxman (2011), we constrained the radius of the exploding star. With an optical opacity of $k = 0.34$ cm^2 g^{-1} the temperature evolution of SN 2013ej is consistent with that of a progenitor with radius 400–600 $R_\odot$.

We remark that no host reddening was assumed in this calculation of the progenitor radius, which is consistent with the lack of Na I D lines at the redshift of M74 in the echelle spectrum obtained with the 1.82 m Asiago telescope (see Fig. 3b). With the addition of some host reddening, the temperature and consequently the radius estimates would be larger.

The likely RSG progenitor star identified by Fraser et al. (2013) has a luminosity of $\log L/L_\odot = 4.5$–4.9 dex, which would imply radii of 400–800 $R_\odot$ for M-type supergiant stellar effective temperatures. These radii are also consistent with that of the Type IIP

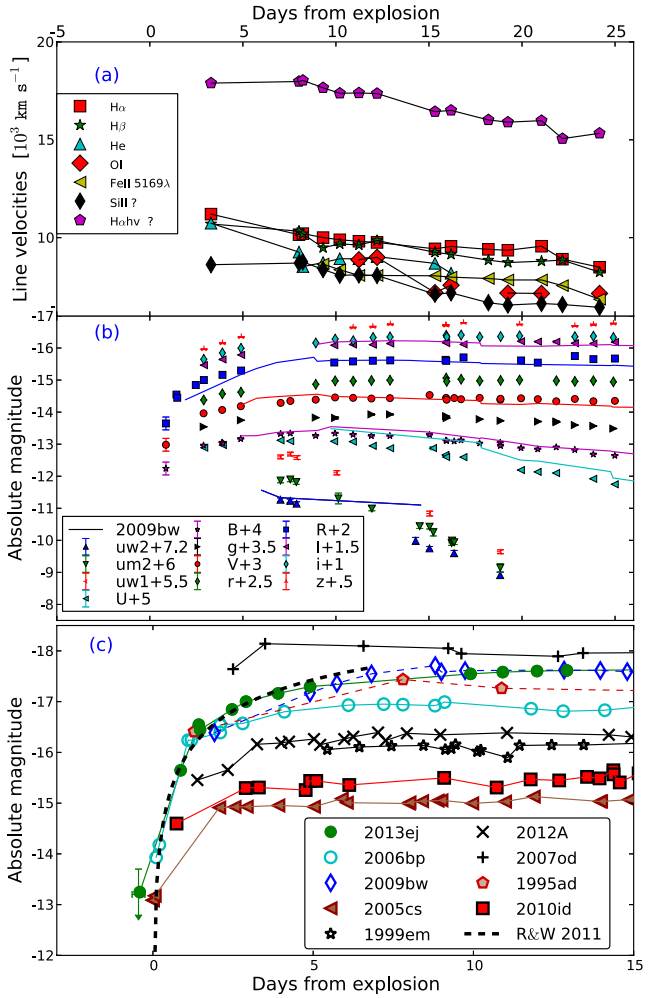

Figure 2. (a) Line velocity evolution for different elements in the ejecta of SN 2013ej. (b) Light curves of SN 2013ej in different bands (symbols), and comparison with the light curves of the twin SN 2009bw (solid lines). (c) Absolute *R*-band light curve of SN 2013ej compared with those of other SNe IIP: SN 2006bp (Quimby et al. 2007), SN 2009bw (Inserra et al. 2012), SN 2005cs (Pastorello et al. 2006), SN 2007od (Inserra et al. 2011), SN 2012A (Tomasella et al. 2013), SN 1995ad (Inserra et al. 2013) and SN 2010id (Gal-Yam et al. 2011). *R* light curve for an RSG (radius ∼320–580 $R_{\odot}$) using equations 13 and 14 from Rabinak & Waxman (2011). The explosion epoch has been constrained using the Rabinak & Waxman (2011) model, the pre-explosion non-detection and detections reported in Lee et al. (2013).

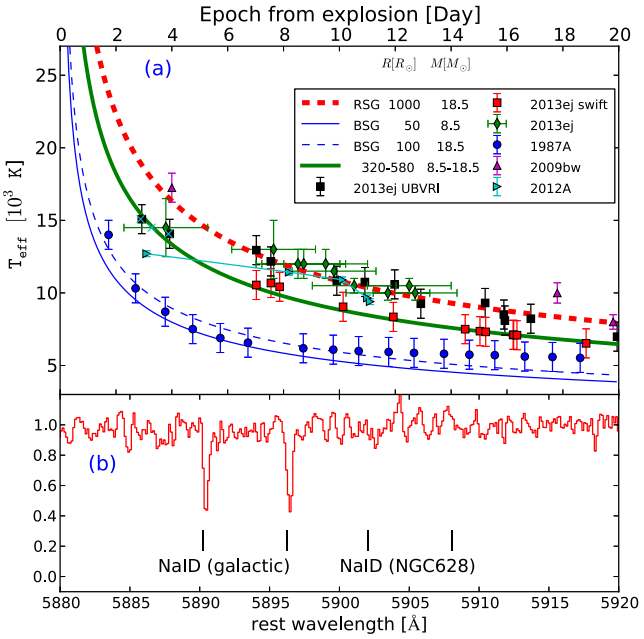

Figure 3. (a) Progenitor radius constraints using Rabinak & Waxman (2011) for RSG (red line), BSG (blue line) and 2013ej best fit (green line). Comparison objects: SN 1987A (Menzies et al. 1987), SN 2012A (Tomasella et al. 2013) and SN 2009bw (Inserra et al. 2012). (b) Echelle spectrum of SN 2013ej obtained at the 1.8 m Asiago telescope on 2013 August 24. The Galactic Na I D is clearly visible, while no Na I D is detected at the redshift of M74. The *x*-axis is in the observed frame.

SN 2009bw (Inserra et al. 2012), which shares several other characteristics with SN 2013ej, as we will discuss in the next section.

The inferred radius values should be confirmed with more detailed models, but here we may safely conclude that the temperature evolution of SN 2013ej is consistent with that expected in the explosion of an extended progenitor. In Fig. 3(a), we also present progenitor radius constraints for SN 2013ej utilizing our *Swift* and optical broad-band photometry, which generally agree with our spectroscopic results. We note that the temperature evolution inferred using the *Swift* data is always lower than that derived from the optical data, suggesting that some UV line blanketing is already present at very early phases. We further compare the temperature evolution of SN 2013ej with those of other SNe II. The photospheric temperatures and radii of SN 2013ej are similar to those of SN 2009bw and SN 2012A, while they are always higher than those of SN 1987A.

4 DISCUSSION AND CONCLUSION

In this Letter, we present the early photometric and spectroscopic evolution of SN 2013ej, a luminous SN II that exploded in M74. Data were obtained mostly with the 1 and 2 m telescopes of the LCOGT network, complemented with data from the PESSTO collaboration. The most interesting characteristic of our sequence of early-time spectra of SN 2013ej is a prominent absorption on the blue side of the Hα. We interpret it as due to Si II, since there is no evidence of HV hydrogen features in proximity other than Balmer or Paschen lines. This absorption dip is not particularly strong in other *slow-rising* SNe II, although it was detected in SN 2009bw. Inserra et al. (2012) proposed it to be evidence that SN 2009bw was interacting with the H-rich Circumstellar Material (CSM) already at early phases. However, we do not find unequivocal evidence of interaction in SN 2013ej – at least not before 30 d after explosion. Nonetheless, we cannot rule out that signatures of interaction between SN ejecta and CSM may appear at later stages, since this was observed in a number of SNe II (Chugai et al. 2007). SN 2013ej shows an unusually slow rise to the light-curve plateau. This property was observed only in the Type IIP SN 2006bp and SN 2009bw. All of them are more luminous than normal SNe II (Patat et al. 1994), but the statistics accumulated so far are poor. Through modelling (Zampieri et al. 2003; Pumo & Zampieri 2011), Inserra et al. (2012) estimated a progenitor mass of 11–15 $M_{\odot}$ for SN 2009bw. If the early spectroscopic and photometric similarities of SN 2013ej with SN 2009bw are confirmed at late phases, this mass range should also be considered plausible in the case of SN 2013ej,

and consistent with the progenitor mass inferred from the analysis of Fraser et al. (2013).

ACKNOWLEDGEMENTS

AP, LT and SB are partially supported by the PRIN-INAF 2011 with the project 'Transient Universe: from ESO Large to PESSTO'. AG acknowledges support by the EU/FP7 via ERC grant no. 307260, a GIF grant and the Kimmel award. The research of JRM is funded through a Royal Society University Research Fellowship. The Infrared Telescope Facility is operated by the University of Hawaii under Cooperative Agreement no. NNX-08AE38A with the National Aeronautics and Space Administration, Science Mission Directorate, Planetary Astronomy Programme. This Letter is based on observations made with the following facilities: ESO NTT telescope (programme ID 188.D-3003), LCOGT 1 m telescopes (Haleaka, Siding Spring, Cerro Tololo, Mc Donald Observatory), NASA Infrared Telescope Facility (IRTF), 1.8 and 1.2 m telescopes (Asiago).

REFERENCES

Baron E. et al., 2000, AJ, 545, 444
Brown P. J. et al., 2009, AJ, 137, 4517
Brown T. M. et al., 2013, PASP, 125, 1031
Chevalier R. A., Irwin C. M., 2011, AJ, 729, L6
Chugai N. N., Chevalier R. A., Utrobin V. P., 2007, AJ, 662, 1136
Cushing M., Vacca W., Rayner J., 2004, PASP, 116, 362
Dessart L., Hillier D. J., 2006, A&A, 447, 691
Dessart L., Hillier D. J., 2010, MNRAS, 410, 1739
Dhungana G. et al., 2013, CBET, 3609, 2
Fisher A. K., 2000, PhD thesis, Univ. Oklahoma
Fraser M. et al., 2013, preprint (arXiv:1309.4268)
Gal-Yam A. et al., 2011, AJ, 736, 159
Hamuy M. A., 2001, PhD thesis, Univ. Arizona
Inserra C. et al., 2011, MNRAS, 417, 261
Inserra C. et al., 2012, MNRAS, 422, 1122
Inserra C. et al., 2013, A&A, 555, A142
Kim et al., 2013, CBET, 3606, 1
Landolt A. U., 1992, AJ, 104, 340
Lee M. et al., 2013, Astron. Telegram, 5466, 1
Leonard D. C. et al., 2002, PASP, 114, 35
Menzies J. W. et al., 1987, MNRAS, 227, 39 P
Pastorello A. et al., 2006, MNRAS, 370, 1752
Patat F., Barbon R., Cappellaro E., Turatto M., 1994, A&A, 282, 731
Pumo M. L., Zampieri L., 2011, AJ, 741, 41
Quimby R. M., Wheeler J. C., Hoflich P., Akerlof C. W., Brown P. J., Rykoff E. S., 2007, AJ, 666, 1093
Rabinak I., Waxman E., 2011, AJ, 728, 63
Rayner J., Toomey D., Onaka P., Denault A., Stahlberger W., Vacca W., Cushing M., Wang S., 2003, PASP, 115, 362
Roming P. W. A. et al., 2005, Space Sci. Rev., 120, 95
Shappee B. J. et al., 2013, CBET, 5237, 1
Smartt S. J., 2009, ARA&A, 47, 63
Tomasella L. et al., 2013, MNRAS, 434, 1636
Vacca W., Cushing M., Rayner J., 2003, PASP, 115, 389
Valenti S., Sand D., Howell D. A., Graham M. L., Parrent J. T., Zheng W., Cenko B., 2013, CBET, 3609, 1
Waxman E., Meszaros P., Campana S., 2007, AJ, 667, 351
Zampieri L., Pastorello A., Turatto M., Cappellaro E., Benetti S., Altavilla G., Mazzali P., Hamuy M., 2003, MNRAS, 338, 711

SUPPORTING INFORMATION

Additional Supporting Information may be found in the online version of this article:

Table 1. Journal of spectroscopic observations.
Table 2. Photometric Data.
(http://mnrasl.oxfordjournals.org/lookup/suppl/doi:10.1093/mnrasl/slt171/-/DC1).

Please note: Oxford University Press are not responsible for the content or functionality of any supporting materials supplied by the authors. Any queries (other than missing material) should be directed to the corresponding author for the article.

This paper has been typeset from a TEX/LATEX file prepared by the author.